Biomech Model Mechanobiol (2010) 9:551–561
DOI 10.1007/s10237-010-0196-8

ORIGINAL PAPER

Modelling of the provisional side-branch stenting approach for the treatment of atherosclerotic coronary bifurcations: effects of stent positioning

Dario Gastaldi · Stefano Morlacchi · Roberto Nichetti · Claudio Capelli · Gabriele Dubini · Lorenza Petrini · Francesco Migliavacca

Received: 16 June 2009 / Accepted: 25 January 2010 / Published online: 14 February 2010

Abstract The most common approach to treat atherosclerosis in coronary bifurcations is the provisional side-branch (PSB) stenting, which consists sequentially of the insertion of a stent in the main branch (MB) of the bifurcation and a dilatation of the side branch (SB) passing through the struts of the stent at the bifurcation. This approach can be followed by a redilatation of the MB only or by a Final Kissing Balloon (FKB) inflation, both strategies leading to a minor stent distortion in the MB. The positioning of the stent struts in the bifurcation and the stresses generated in the stent and vessel wall are worthy of investigation for a better understanding of the mechanobiology of the system. For this purpose, a computer model of an atherosclerotic coronary bifurcation based on the finite element method was developed; the effects of performing the final redilatation with the two strategies utilising one or two balloons and those created by a different stent strut positioning around the SB were investigated. Results correlate well with previous experimental tests regarding the deformation following balloon expansion. Furthermore, results confirm firstly that the re-establishment of an optimal spatial configuration of the stent after the PSB approach is achieved with both strategies; secondly, results show that case of stent positioning with one cell placed centrally (with regard to the SB) should be preferred, avoiding the presence of struts inside the vessel lumen, which may reduce hemodynamic disturbances. The central positioning also resulted in a better solution in terms of lower stresses in the stent struts and, more importantly, in the vascular tissues.

Keywords Stent · Balloon · Arterial tissue · Bifurcation · Finite element method

D. Gastaldi · S. Morlacchi · R. Nichetti · G. Dubini · L. Petrini · F. Migliavacca (✉)
Laboratory of Biological Structure Mechanics,
Structural Engineering Department, Politecnico di Milano,
Piazza Leonardo da Vinci, 32, 20133 Milano, Italy
e-mail: francesco.migliavacca@polimi.it
URL: http://www.labsmech.polimi.it

C. Capelli
Cardiac Unit, Institute of Child Health and Great Ormond Street Hospital, University College of London, London, UK

1 Introduction

The most common interventional technique used to restore blood flow in stenotic coronary arteries consists of implantation of tubular metallic structures in pathological vessels. These devices, known as stents, have shown excellent clinical outcomes in non-bifurcated vessels, particularly after the introduction of drug-eluting stents (DES). Indeed, DES when properly used are able to avoid restenosis, identified as the main cause of failure for these procedures (Morice et al. 2002; Moses et al. 2006). However, stent implantation in complex geometries such as coronary bifurcations remains a challenging clinical problem, with a high rate of procedural complications (Colombo et al. 2004).

Different techniques (crush technique, culotte technique, T-stenting, V-stenting, etc.) that imply the insertion of two or more devices are described in the literature (Iakovou and Colombo 2005). All of these methodologies have specific pros and cons. For example, the crush and culotte techniques create zones on the vessel wall with multiple metallic layers increasing the possibility of thrombosis generation; to overcome this limitation, other techniques, such as T-stenting, do not entirely cover the coronary wall, with negative consequences on the drug-eluting dynamics and subsequent therapeutic success. Moreover, techniques involving two or more stents require a longer interventional time resulting in higher angiographic contrast dose and exposure to radiation.

These limitations have made provisional side-branch (PSB) stenting the current preferred strategy. This consists of the implantation in the main branch (MB) of only one stent with the drawback of limiting subsequent access to the side branch (SB) because of interposition of the device structures. In order to restore the SB patency, the expansion of a balloon through the stent struts is required. This process improves the hemodynamic conditions and provides the possibility of crossing the struts with another device if the immediate clinical results are unsatisfactory but at the same time induces stent distortion in the MB. This drawback was studied by Ormiston et al. (1999) with in vitro experiments, which demonstrated that main stent lumen compromise can be abolished by main lumen redilatation or by simultaneous expansion of two balloons (Final Kissing Balloon, FKB) in the MB and SB vessels as final step. Furthermore, those authors affirmed that the FKB ensures the maintenance of both main and side-branch lumens providing a slightly larger side-lumen diameter, and the FKB allows an easier access for the delivery of a second device in the SB. However, the FKB provides also some drawbacks, among which the most important is certainly a highest stress field on the arterial wall. As a consequence of the debate on the use of one or two balloons this final step is still open (Sheiban et al. 2009). In addition to in vitro tests, computer models (Liang et al. 2005; Lally et al. 2005; Wu et al. 2007; Kiousis et al. 2007; Gijsen et al. 2008; Pericevic et al. 2009; Capelli et al. 2009; Zunino et al. 2009) are able to examine different stenting techniques with lower costs and are a significant research tool for both physicians and industry. Indeed, computer methods can provide accurate information on stent expansion and also estimate mechanical stresses on the biological tissues interacting with the stents.

In the literature, Mortier et al. (2009a,b) used finite element analyses to study the stenting procedure in coronary bifurcations. In their studies, the authors observed the behaviour of different stent designs in terms of strut distortion at the SB access after balloon dilation (Mortier et al. 2009a) and compared three different stents in the curved main branch of a coronary bifurcation with the aim of providing better insights into the related changes of the mechanical environment (Mortier et al. 2009b).

The aim of the present study is the implementation of a numerical model able to analyze through the finite element method the stent behaviour in applications involving coronary bifurcations. In particular, we investigate the PSB approach focusing the attention (1) on the effects of three different accesses to the SB and (2) on the comparison between the FKB procedure and the redilatation of the MB only as final step of the interventional procedure. The model describing the PSB-stenting approach includes the interactions between the balloons, the arterial wall and the atherosclerotic plaques; furthermore, it describes the mechanical behaviour of biological tissues with a nonlinear stress–strain relationship, which takes into account the three different layers of the coronary wall. The stress state generated both in the stent and in the vessel tissues by the interaction between the stent, the balloons and the arterial bifurcation is thoroughly investigated in relation to the different stent struts positioning in proximity to the side branch and the final simulated interventional option.

2 Materials and methods

2.1 Atherosclerotic coronary bifurcation

The bifurcation geometry was identified by the angle of intersection (70°), the internal diameter of the MB (2.78 mm), the internal diameter of the SB (2.44 mm), the thickness of the wall (0.9 mm, assumed to be uniform throughout the model), the length of the MB (47 mm) and the length of the SB (22.5 mm, Fig. 1). The arterial wall was divided into three layers with different thicknesses corresponding to intima (0.24 mm), media (0.32 mm) and adventitia (0.34 mm) according to the data obtained by Holzapfel et al. (2005). Atherosclerotic plaques were modelled with a length of 3.9 mm in the MB and 4.3 mm in the SB, and a width of 0.5 mm and placed in the bifurcation in accordance with the Medina (1,1,1) classification (Medina et al. 2006) with the presence of stenoses both in the proximal and distal part of the MB and in the SB (60% area reduction in the MB and 65% in the SB, respectively).

A hyperelastic isotropic constitutive law, suitable for nearly incompressible materials accounting for large strains, was adopted for the arterial layers in accordance with the experimental data obtained by Holzapfel et al. (2005) in stress–strain tests in the circumferential direction. The adopted constitutive law was based on a sixth-order reduced polynomial strain energy density function:

$$U = C_{10}(\bar{I}_1 - 3) + C_{20}(\bar{I}_1 - 3)^2 + C_{30}(\bar{I}_1 - 3)^3 + C_{40}(\bar{I}_1 - 3)^4 + C_{50}(\bar{I}_1 - 3)^5 + C_{60}(\bar{I}_1 - 3)^6 \quad (1)$$

where C_{i0} are the material parameters (Table 1) and $\bar{I}_1$ is the first deviatoric strain invariant defined as:

$$\bar{I}_1 = \bar{\lambda}_1^2 + \bar{\lambda}_2^2 + \bar{\lambda}_3^2$$

with the deviatoric stretches $\bar{\lambda}_i$ related to the principal stretches λi and total volume ratio J by the relation

$$\bar{\lambda}_i = J^{-1/3}\lambda_i.$$

With the aim of approximately describing the mechanical failure of an atherosclerotic plaque, its material was described coupling an isotropic hyperelastic model with a plasticity model: it allows consideration of stenosis reduction after stent expansion and arterial elastic recoil. The hyperelastic part of the stress–strain curve was implemented using

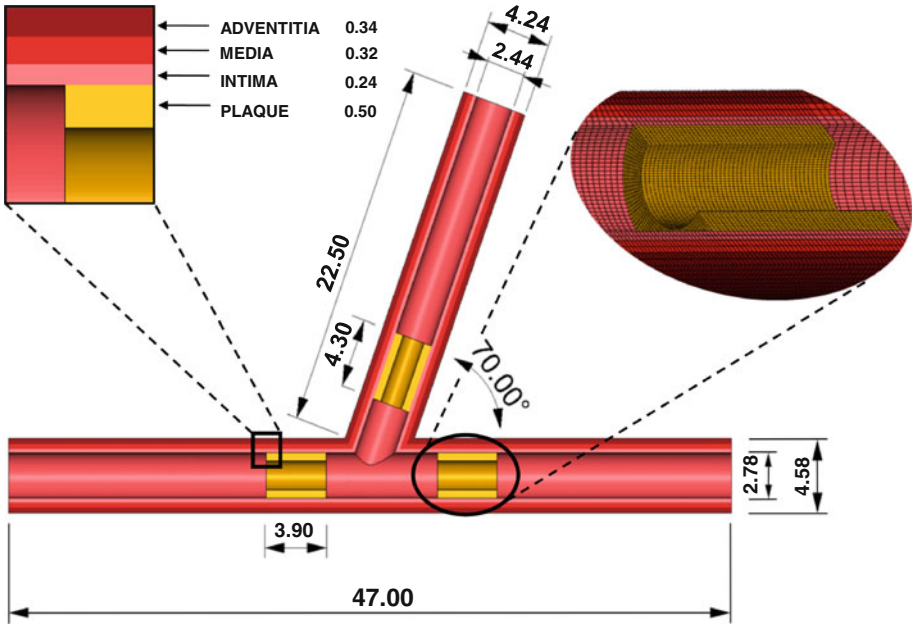

Fig. 1 Geometric model of the atherosclerotic bifurcation. In the *upper left* magnification area, the thicknesses of arterial wall layers and of atherosclerotic plaque are depicted. In the *upper right* magnification area, a detail of the mesh is reported: eight rows of elements in circumferential direction are visible for the plaque and six for the arterial wall, two for each layer. Dimensions are in millimetres

Table 1 Coefficients of strain energy density function for the coronary bifurcation

	C_{10} [MPa]	C_{20} [MPa]	C_{30} [MPa]	C_{40} [MPa]	C_{50} [MPa]	C_{60} [MPa]
Intima	6.79E−03	5.40E−01	−1.11	10.65	−7.27	1.63
Media	6.52E−03	4.89E−02	9.26E−03	0.76	−0.43	8.69E−02
Adventitia	8.27E−03	1.20E−02	5.20E−01	−5.63	21.44	0.00
Plaque	2.38E−03	1.89E−01	−3.88E−01	3.73	−2.54	5.73E−01

the strain energy density function (1) in which the parameters C_{i0} (Table 1) were modified to describe the stress–strain curve obtained by Loree et al. (1994) for cellular plaques. For strain values greater than 34%, a perfect plasticity model was assumed for the plaque response. The stress plateau value was fixed at 0.4 MPa, accordingly with the rupture stress registered by Loree et al. (1994). A density value of 1120 kg/m^3 was used. Artery and plaques were meshed using about 360,000 reduced-integration 8-node cubic elements (Fig. 1). The accuracy of the mesh density used in the analyses is guaranteed by the mesh sensitivity study performed by the authors and published in a recent paper (Capelli et al. 2009) on a similar arterial wall.

2.2 Stent

The Cordis BX Velocity stent (Johnson & Johnson Interventional System, Warren, NJ, USA) already used in previous studies (Gervaso et al. 2008; Capelli et al. 2009) was employed (Fig. 2a). The stent geometry was reconstructed from optical microscopy images (Migliavacca et al. 2005). The length, the internal diameter and the strut thickness in the crimped configuration were 17.7, 0.9, and 0.14 mm, respectively (Fig. 2a). The stent material was stainless steel AISI 316L. The elasto-plastic behaviour of this material was described through a Von Mises-Hill plasticity model with isotropic hardening. Other parameters used were Young modulus (193 GPa), Poisson ratio (0.3), yield stress (205 MPa), ultimate stress (515 MPa), ultimate deformation (60%) and material density (8000 kg/m^3). The stent geometry discretization resulted in a highly regular mesh of about 67,000 8-node cubic elements with reduced integration (Fig. 2b), which respects the results of the sensitivity analysis performed by Capelli et al. (2009) on the same model.

2.3 Balloon

A polymeric balloon was modelled with an inflated diameter of 3 mm (Fig. 2c). Membrane elements with a thickness of 0.03 mm were used to discretize the balloon. A preliminary analysis, in which a negative pressure of 0.01 MPa was applied to the balloon's inner surface, was performed to obtain the deflated configuration (Fig. 2d). Once deflated, the balloon was inserted in the stent (Fig. 2e). To simulate the FKB and the access to the SB, a stress-free bended balloon configuration was needed. This was created applying

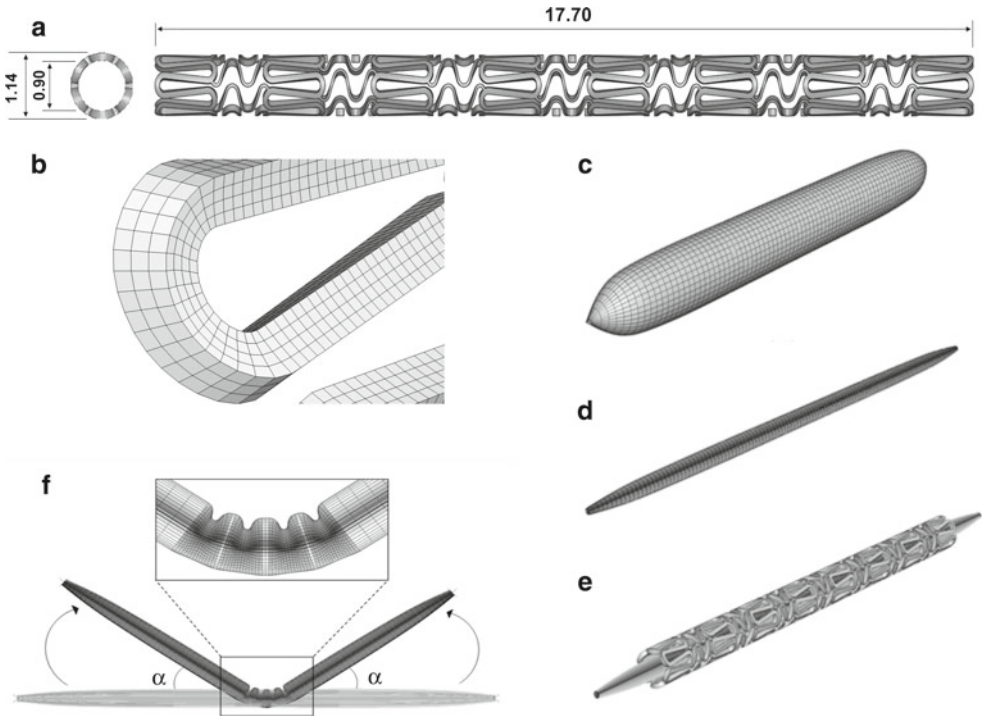

Fig. 2 **a** CAD model of stent Cordis BX Velocity with the dimensions of length, external and internal diameters reported in millimetres; **b** particular of the mesh of the stent; **c**, **d**, **e**, **f** the balloon inflated and deflated configurations (see text)

rotations to the tops of the balloon (Fig. 2f). The bending angles were 70° for the access to the SB, and 60° and 10° for the FKB. During the simulations, balloons were constrained at the ends fixing only the radial direction. In such a way, longitudinal and circumferential degrees of freedom are not constrained.

The polymer was modelled as an isotropic, linear-elastic material providing a semi-compliant behaviour to the balloon (E = 1,455 MPa and $\nu = 0.3$). The material density was 1256 kg/m^3. The geometry was discretized with 4-node membrane elements: the mesh consists of about 5,700 elements for the balloon in the MB and about 18,000 for the balloon in the SB (Fig. 2c).

2.4 Simulations

Due to the high nonlinearity of this problem (mainly a result of the nonlinear material behaviour and complex contact conditions), we performed a quasi-static analysis using an explicit dynamics procedure: the commercial code ABAQUS/Explicit (Simulia Corp., RI, USA) was adopted. Because the explicit integration method (central difference rule) is conditionally stable, specific attention has to be paid to time increment size that depends mainly on the characteristic element length, material constitutive parameters and density. In this work, to follow a cost-saving approach maintaining solution accuracy, an element-by-element stable time increment estimate coupled with a "variable mass scaling technique" was used, allowing an ad hoc adjustment of the material density in space and simulation time (ABAQUS 2008). Analysis time-step and loading rate were adequate to ensure a static equilibrium along the analysis. The quasi-static regime was verified by a ratio between kinetic and internal energy lower than 5% (Fig. 3).

Contacts between parts of the model were defined according to the general contact algorithm available in ABAQUS/Explicit.

The PSB-stenting procedure was simulated in six different steps (Fig. 4):

1. Positioning of the delivery system (balloon and stent) inside the coronary bifurcation (Fig. 4a).
2. Expansion of the stent in the MB by application of a pressure of 1 MPa on the internal surface of the balloon (Fig. 4b).
3. Deflation of the MB balloon to measure the elastic recoil of the system (Fig. 4c).
4. Positioning of the SB balloon through the stent struts (Fig. 4d).
5. Dilatation of the stent cell in proximity to the bifurcation by application of 1 MPa pressure on the internal surface of the 70° deflected balloon (Fig. 4e).

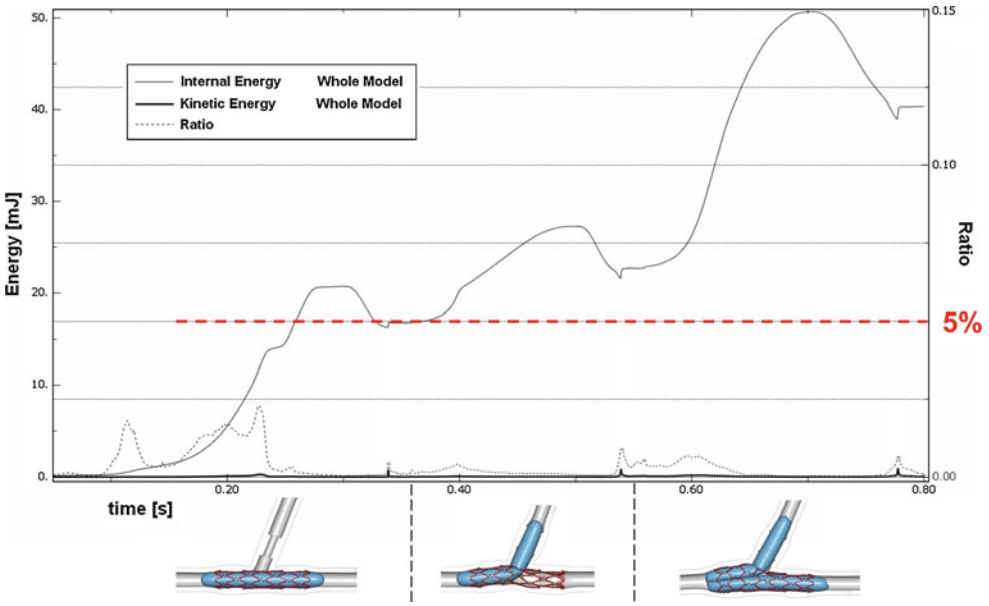

Fig. 3 Plot of the kinetic (*thick solid line*), internal (*thin solid line*) energies and their ratio (*dotted line*) for the whole model during the entire simulation

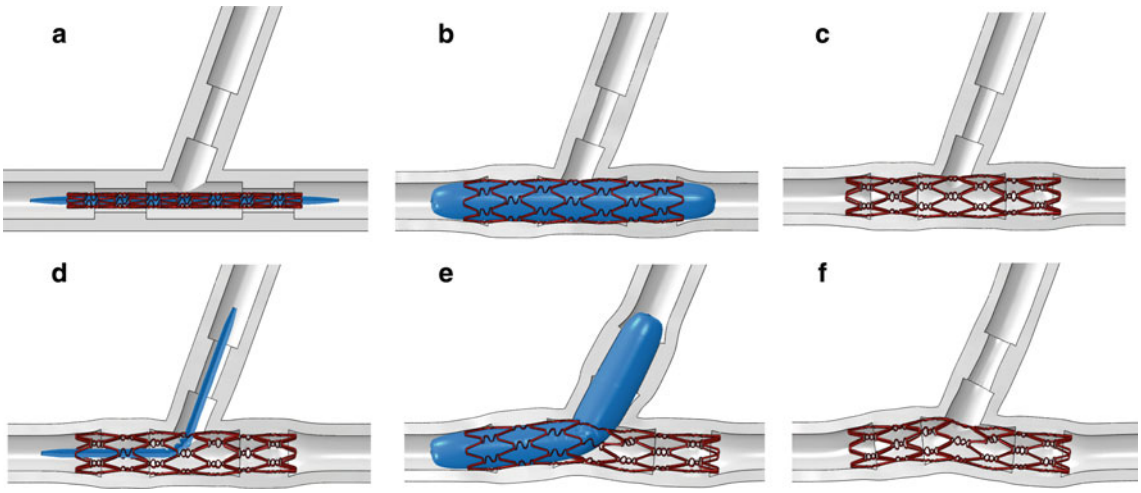

Fig. 4 Provisional side-branch-stenting simulation steps. Initial position (**a**), balloon expansion (**b**) and recoil (**c**) of the system in the MB. Insertion of a balloon in the SB through a cell of the stent (**d**), balloon expansion (**e**) and elastic recoil of the system (**f**)

6. Deflation of the SB balloon (Fig. 4f).

Since this procedure is highly affected by the stent position in the MB, which is only under limited control of the operator during the implantation, three different simulations were performed:

Case 1. Stent positioned with one cell placed centrally with regard to the side branch (Fig. 5a);
Case 2. Stent placed in order to cross the cell proximally (Fig. 5b);
Case 3. Stent placed in order to cross the cell distally (Fig. 5c).

Subsequently, starting from the final configuration of Case 1 (central access), two analyses investigating the potential final steps were performed (Fig. 6):

Case 1A. Simultaneous expansion and deflation of two balloons in each of the branches of the bifurcation (FKB) by application of a pressure of 1 MPa (Fig. 6a).
Case 1B. Redilatation of a 3.0- mm balloon in the MB only by application of a pressure of 1 MPa (Fig. 6b).

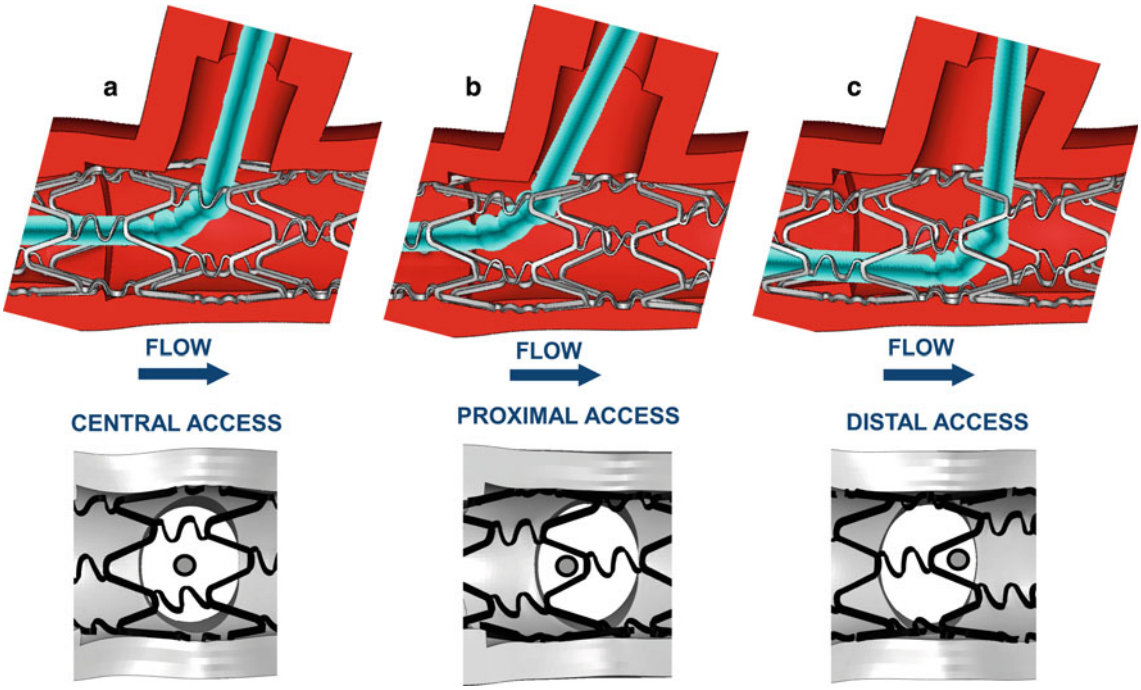

Fig. 5 Access to the SB for three different stent positions. *Lower panel* views towards the SB; the *grey circle* shows the balloon position; *Upper panel* frontal views. **a** central access; **b** proximal access; **c** distal access

3 Results and discussion

Stress and deformation fields on the artery, plaque and stent were evaluated for each PSB stenting simulation performed.

Solutions obtained in terms of stent deformations were compared to the results of an experimental test (Ormiston et al. 2006) to determine the device distortions after expansion of the balloon in the SB and after the FKB (Fig. 7). The similarity between the two solutions provides a first qualitative validation of the implemented model.

From a quantitative point of view, analyses regarding residual stenosis (RS), equivalent plastic strains (PEEQ), stresses in the stent and the arterial wall are outlined in the following paragraphs for case 1A (central access and Final Kissing Balloon), together with some geometrical considerations concerning the comparisons between the three accesses to the SB and between the two final steps for the restoration of the main vessel lumen.

The efficacy of stenting is generally evaluated in terms of RS. For the investigated case, the stenting technique almost provided total recovery of the lumen (RS $< 1\%$).

The PEEQ maps of a proximal part of the stent after the expansion of the device in the MB and after the FKB for case 1A (stent positioned with one cell placed centrally with regard to the side branch and FKB inflation) are shown in Fig. 8. As expected, the inelastic behaviour is concentrated in the curved portions of the rings, where plastic hinges are developed to allow expansion of the device. The maximum PEEQ values are around 20% after expansion of the device in the MB, while they reach values up to 34% after the FKB. Even if this value of plastic strain is far from the ultimate deformation of stainless steel (around 60%), it is evident that the FKB procedure is very demanding for the stent. Accordingly, particular attention has to be paid to the selection of the material used for producing the stent as well as in the build-up of plastic strain during crimping. The highest stress values in the stent vary between 410 MPa after the expansion in the MB and 490 MPa at the end of the procedure.

To analyze the stress field in the artery, maximum principal stress maps of the vascular wall and the plaques developed during the procedure for central stent positioning (case 1A) are shown in Fig. 9. The greatest stresses can be found in the proximal part of the MB and in the proximity of the carina during the FKB.

This unfavourable situation in terms of stresses and strains after the FKB is also visible in Fig. 6 where the two different final steps are compared. Both the FKB and the MB redilatation are able to restore an optimal spatial configuration in the MB for the device; but in the first procedure, the simultaneous presence of two balloons results in higher stresses in the arterial wall. Moreover, SB access in terms of projected cell area seems not to be greatly affected by the final step performed confirming Ormiston results

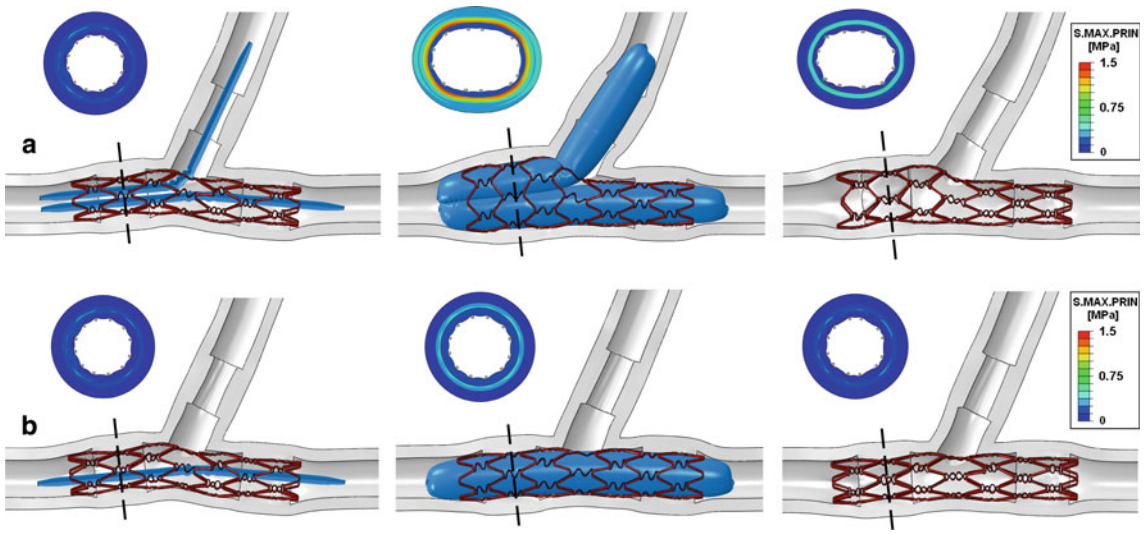

Fig. 6 Final step strategies after the SB access. **a** FKB procedure: insertion of two balloons, simultaneous expansion and elastic recoil. **b** Dilatation of the MB only: insertion of one balloon in the MB, expansion and elastic recoil. Cross-sections show maximum principal stresses in the arterial wall during the different steps of the procedures

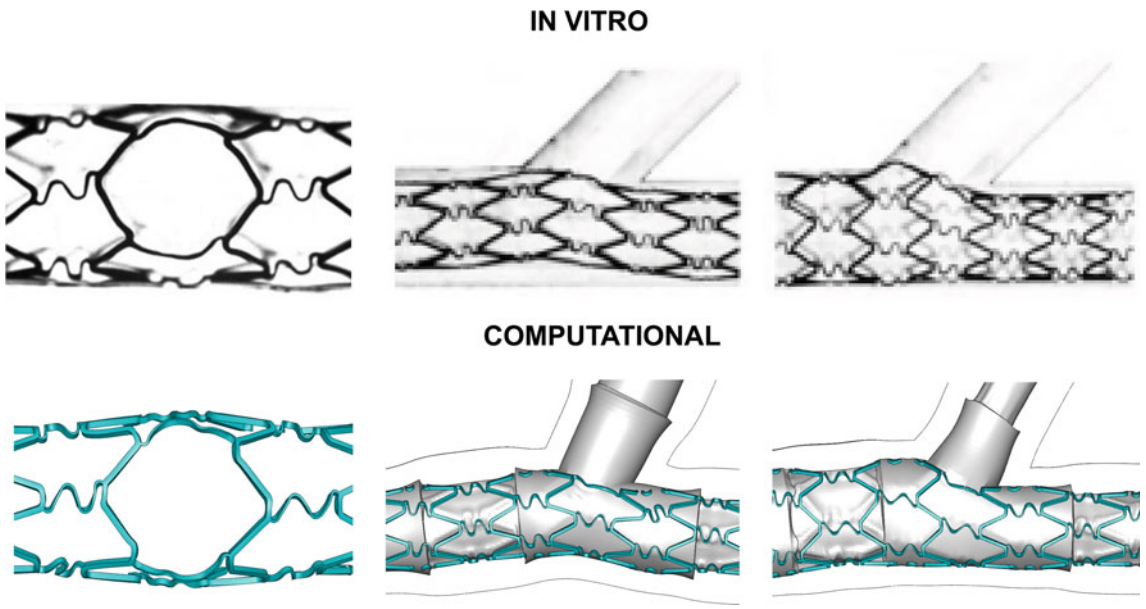

Fig. 7 Comparison between the results of the experimental data (*top*, modified by Ormiston et al. 2006) and of the computational analysis (*bottom*). *Left and centre* the results after the SB stenting in two different views; *right* the configurations after the FKB

(Ormiston et al. 1999). Therefore, these considerations corroborate from a mechanical point of view that the redilatation of the MB should be preferred as a final step after a PSB approach.

Analyzing the different SB accesses, Fig. 10 shows the distortion angles of the device in the MB and the stent struts in proximity to the bifurcation after the SB access. The expanded balloon allows an access to the SB free from stent struts only in the central case where the projected cell area available for the blood flow is the 79.8% of the total lumen area. In the proximal and distal cases, the amounts of the three areas (57.4, 8.2, 9.9 for the proximal access; 21.5, 25.7, 28.6 for the distal access) are, respectively, 75.5 and 75.8%. Considering the absence of stent struts protruding into the branches in the central positioning, minor hemodynamic implications after the procedure are expected. Furthermore, with distal and proximal access to the SB, a higher stress field and higher plastic deformations can be found both in the stent (Fig. 10, bottom) and in the intimal layer of the arterial wall (Fig. 11).

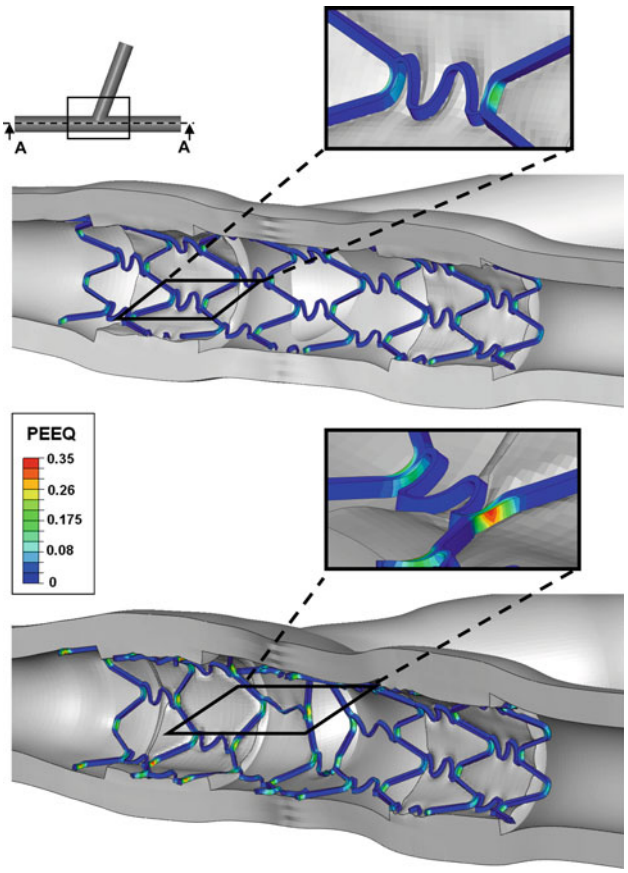

Fig. 8 Equivalent plastic strains in the stent after the MB stenting (*top*) and the FKB (*bottom*)

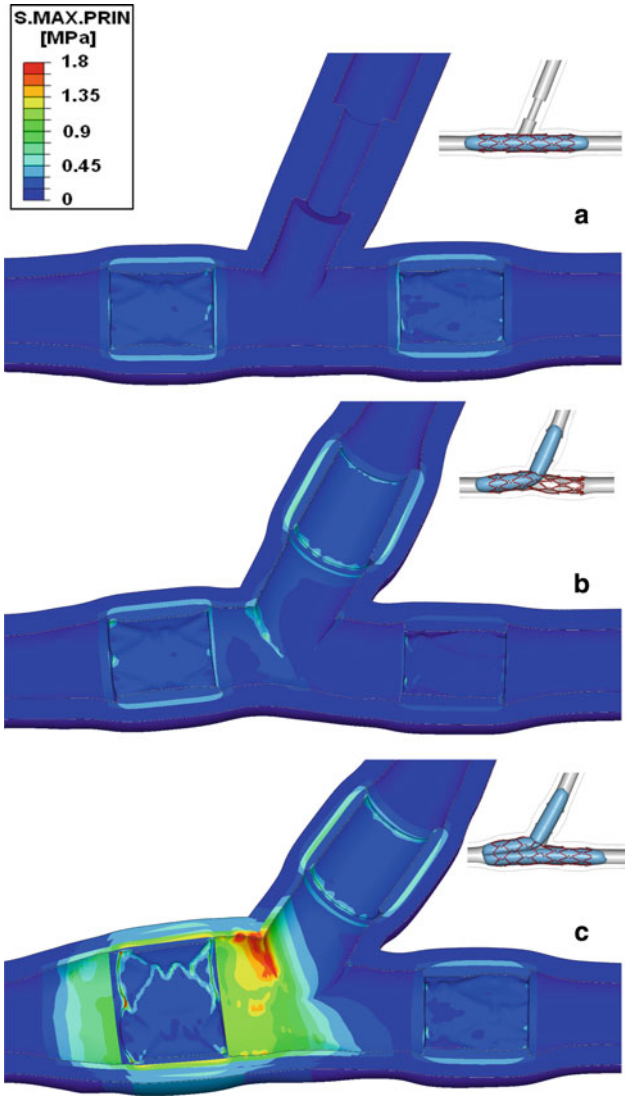

Fig. 9 Maximum principal stress colour maps in the arterial wall after the three steps of the procedure in case 1A

3.1 Limitations

The main limitation of this work is the description of biological tissue constitutive laws. More advanced constitutive models are available in the literature taking into account the anisotropy related to fibre dispersion in the tissue (Gasser and Holzapfel 2007; Hariton et al. 2007; Gasser et al. 2006). However, in order to apply these more complex constitutive models, parameters calibration is a crucial issue. Precise information about fibre orientation in the bifurcated region as well as the properties of the plaques are required; they are sensitive to the specific patient and impossible to obtain from routine clinical exams.

An additional limitation of our model is the absence of any rupture mechanism in the arterial components. This limitation has effects on the absolute values of the stresses and deformations of the arterial layers. However, the adopted simplified constitutive relations are an efficient and simple comparative framework to estimate the non-physiological state created by the insertion of a stent with multiple balloon expansions. Indeed, results can be useful to evaluate the vessel zones more prone to damage and hence more subjected to the restenosis process.

An additional limitation of this study is related to plaque geometry and location, which are idealized. Simulations with patient-specific geometries obtained by medical imaging or less idealized plaque geometry would certainly improve the implemented model.

Lastly, other aspects concerning the arterial wall conditions, such as luminal blood pressure, pre-stretch and residual stresses were neglected.

4 Conclusions

Numerical simulations are a very useful and adaptable tool completing and integrating experimental tests for medical device design and evaluation. Ormiston et al. (1999, 2006, 2008) created in vitro tests to study device behaviour during

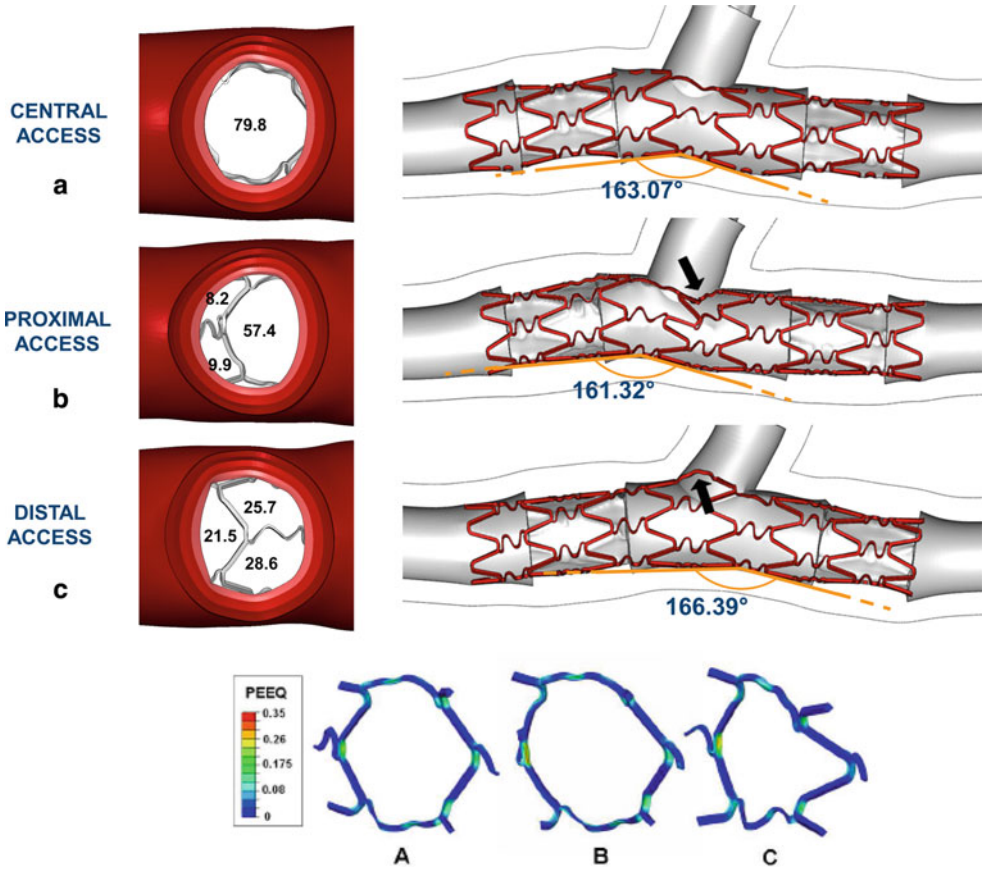

Fig. 10 Stent struts in proximity of the bifurcation after SB access in three cases of stent positioning in the MB. *Numbers* represent the percentage of the projected cell area free from struts. Equivalent plastic strains and the final configurations of the enlarged strut are reported at the bottom. *Arrows* indicate the protrusion of the stent struts in the MB (proximal access) and in the SB (distal access) after the SB access. Angles of distortion of the stent in the MB are reported

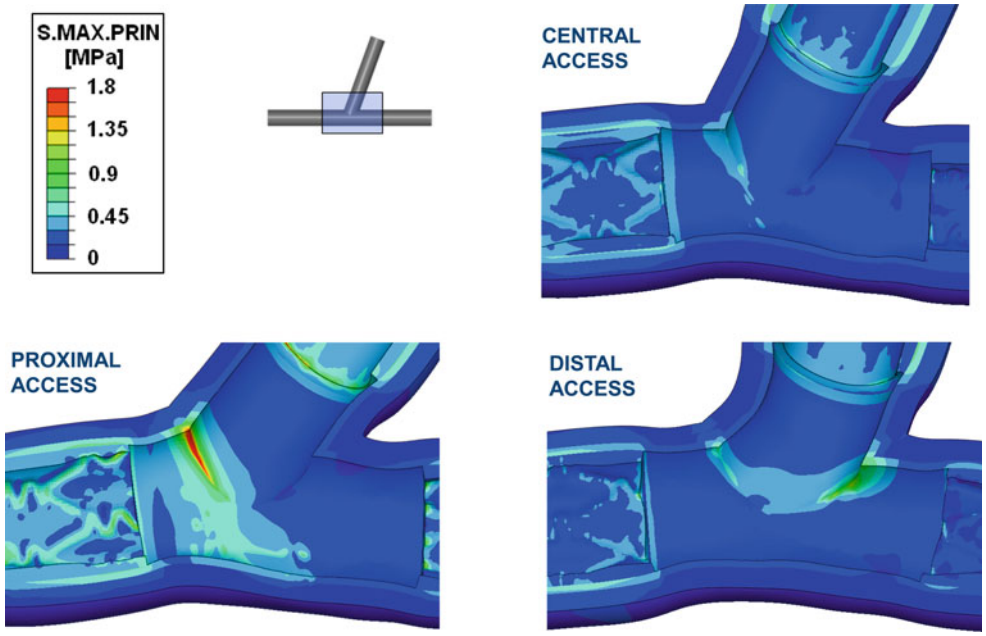

Fig. 11 Maximum principal stress colour maps in the arterial wall during the SB access for central, proximal and distal access to the SB

a bifurcation dedicated treatment. The phantoms they used to simulate the coronary bifurcation are built in plexyglass (Ormiston et al. 1999, 2006), a rigid material with a very different behaviour from the vessel wall or in silicone (Ormiston et al. 2008), a family of deformable polymers. In contrast, the numerical model implemented in our work considered the non-linear aspects for the mechanical properties of the three arterial wall layers, conscious that this constitutive modelling remains a simplification of the reality. Furthermore, the final kissing balloon expansion added an innovation to the stent modelling arena.

Further developments might simulate the behaviour of different stent designs considering other stenting procedures and, more importantly, might also involve fluid dynamics analyses (Balossino et al. 2008; Zunino et al. 2009) to evaluate the whole efficacy of these procedures. The novelty of this computer methodology is its capability of analyzing different stenting techniques dedicated to bifurcation lesions; in the future, computer models similar to those herewith proposed will increase technical knowledge to allow stent designers to obtain information for the optimization of the devices used in bifurcations and clinicians to have some patient-specific proposals for intervention planning.

Acknowledgments This work has been partially supported by the Italian Institute of Technology (IIT, Genoa, Italy), within the project "Models and methods for degradable materials" and by the Fondazione Cassa di Risparmio di Trento e Rovereto.

References

ABAQUS (2008) Analysis user's manual, ver. 6.7EF

Balossino R, Gervaso F, Migliavacca F, Dubini G (2008) Effects of different stent designs on local heamodynamics in stented arteries. J Biomech 41:1053–1061

Capelli C, Gervaso F, Petrini L, Dubini G, Migliavacca F (2009) Assessment of tissue prolapse after balloon expandable stenting: influence of stent cell geometry. Med Eng Phys 31:441–447

Colombo A, Moses JW, Morice MC, Ludwig J, Holmes DR Jr, Spanos V, Louvard Y, Desmedt B, Di Mario C, Leon MB (2004) Randomized study to evaluate sirolimus-eluting stents implanted at coronary bifurcation lesions. Circulation 109:1244–1249

Gasser TC, Holzapfel GA (2007) Modeling plaque fissuring and dissection during balloon angioplasty intervention. Ann Biomed Eng 35:711–723

Gasser TC, Ogden RW, Holzapfel GA (2006) Hyperelastic modelling of arterial layers with distributed collagen fibre orientations. J R Soc Interf 3:15–35

Gervaso F, Capelli C, Petrini L, Lattanzio S, Di Virgilio L, Migliavacca F (2008) On the effects of different strategies in modelling balloon-expandable stenting by means of finite element method. J Biomech 41:1206–1212

Gijsen FJH, Migliavacca F, Schievano S, Socci L, Petrini L, Thury A, Wentzel JJ, van der Steen AF, Serruys PW, Dubini G (2008) Simulation of stent deployment in a realistic human coronary artery. Biomed Eng Online Aug 6, 7:23

Hariton I, DeBotton G, Gasser TC, Holzapfel GA (2007) Stress-modulated collagen fiber remodeling in a human carotid bifurcation. J Theor Biol 248:460–470

Holzapfel GA, Sommer G, Gasser CT, Regitnig P (2005) Determination of layer-specific mechanical properties of human coronary arteries with nonatherosclerotic intimal thickening and related constitutive modeling. Am J Physiol Heart Circ Physiol 289:H2048–H2058

Iakovou I, Colombo A (2005) Contemporary stent treatment of coronary bifurcations. J Am Coll Cardiol 46:1446–1455

Kiousis D, Gasser T, Holzapfel GA (2007) A numerical model to study the interaction of vascular stents with human atherosclerotic lesions. Ann Biomed Eng 35:1857–1869

Lally C, Dolan F, Prendergast PJ (2005) Cardiovascular stent design and vessel stresses: a finite element analysis. J Biomech 38:1574–1581

Liang DK, Yang DZ, Qi M, Wang WQ (2005) Finite element analysis of the implantation of a balloon-expandable stent in a stenosed artery. Int J Cardiol 104:314–318

Loree HM, Tobias BJ, Gibson LJ, Kamm RD, Small DM, Lee RT (1994) Mechanical properties of model atherosclerotic lesion lipid pool. Arterioscler Thromb Vasc Biol 14:230–234

Medina A, de Lezo JS, Pan M (2006) A new classification of coronary bifurcation lesion. Rev Esp Cardiol 59:183–184

Migliavacca F, Petrini L, Montanari V, Quagliana I, Auricchio F, Dubini G (2005) A predictive study of the mechanical behaviour of coronary stents by computer modeling. Med Eng Phys 27:13–18

Morice MC, Serruys PW, Sousa JE, Fajadet J, Ban Hayashi E, Perin M, Colombo A, Schuler G, Barragan P, Guagliumi G, Molnar F, Falotico R (2002) A randomized comparison of a sirolimus-eluting stent with a standard stent for coronary revascularization. N Engl J Med 346:1773–1780

Mortier P, De Beule M, Van Loo D, Verhegghe B, Verdonck P (2009a) Finite element analysis of side branch access during bifurcation stenting. Med Eng Phys 31:434–440

Mortier P, Holzapfel GA, De Beule M, Van Loo D, Taeymans Y, Segers P, Verdonck P, Verhegghe B (2009b) A novel simulation strategy for stent insertion and deployment in curved coronary bifurcations: comparison of three drug-eluting stents. Ann Biomed Eng [Epub ahead of print]

Moses JW, Nikolsky E, Mehran R, Cambier PA, Bachinsky WB, Leya F, Kuntz RE, Popma JJ, Schleckser P, Wang H, Cohen SA, Leon MB (2006) SIRIUS 2.25 investigators. Safety and efficacy of the 2.25-mm sirolimus eluting Bx velocity stent in the treatment of patients with de novo native coronary artery lesions: the SIRIUS 2.25 trial. Am J Cardiol 98:1455–1460

Ormiston JA, Webster MWI, Ruygrok PN, Stewart JT, White HD, Scott DS (1999) Stent deformation following simulated side branch dilatation: a comparison of five stent design. Catheter Cardiovasc Interv 47:258–264

Ormiston JA, Webster MWI, Seifeddin ELJ, Ruygrok PN, Stewart JT, Scott D, Currie E, Panther MJ, Shaw B, O'Shaughnessy B (2006) Drug-eluting stents for coronary bifurcations: bench testing of provisional side-branch strategies. Catheter Cardiovasc Interv 67:49–55

Ormiston JA, Webster MWI, Webber B, Stewart JT, Ruygrok PN, Hatrick RI (2008) The "crush" technique for coronary artery bifurcation stenting: insight from micro-computed tomographic imaging of bench deployment. JACC Cardiovasc Interv 1:351–357

Pericevic I, Lally C, Toner D, Kelly DJ (2009) The influence of plaque composition on underlying arterial wall stress during stent expansion: the case for lesion-specific stents. Med Eng Phys 31:428–433

Sheiban I, Omedè P, Biondi-Zoccai G, Moretti C, Sciuto F, Trevi GP (2009) Update on dedicated bifurcation stents. J Interv Cardiol 22:150–155

Wu W, Wang WQ, Yang DZ, Qi M (2007) Stent expansion in curved vessel and their interactions: a finite element analysis. J Biomech 40:2580–2585

Zunino P, D'Angelo C, Petrini L, Vergara C, Capelli C, Migliavacca F (2009) Numerical simulation of drug eluting coronary stents: mechanics, fluid dynamics and drug release. Comput Method Appl Mech Eng 198(45–46):3633–3644. doi:10.1016/j.cma.2008.07.019